



Growth and optical properties of solid solution crystals $\text{GaSe}_{1-x}\text{S}_x$



K.A. Kokh ^{a, b, c, *}, J.F. Molloy ^d, M. Naftaly ^d, YuM. Andreev ^{c, e}, V.A. Svetlichnyi ^c, G.V. Lanskii ^{c, e}, I.N. Lapin ^c, T.I. Izaak ^c, A.E. Kokh ^a

^a Institute of Geology and Mineralogy, SB RAS, Novosibirsk, Russia

^b Novosibirsk State University, Novosibirsk, Russia

^c Siberian Physical–Technical Institute of Tomsk State University, Tomsk, Russia

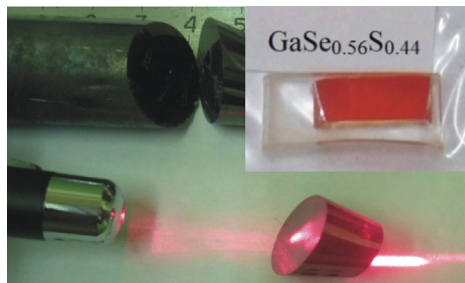
^d National Physical Laboratory, Teddington TW11 OLW, UK

^e Institute of Monitoring of Climatic and Ecological Systems SB RAS, Tomsk, Russia

HIGHLIGHTS

- $\text{GaSe}_{1-x}\text{S}_x$ crystals were grown.
- 3 weight % of S is optimal.
- Absorption anisotropy decreases with doping.

GRAPHICAL ABSTRACT



ARTICLE INFO

Article history:

Received 4 August 2014

Received in revised form

26 January 2015

Accepted 28 January 2015

Available online 3 February 2015

Keywords:

A. Electronic materials

B. Crystal growth

C. Optical properties

ABSTRACT

$\text{GaSe}_{1-x}\text{S}_x$ ($x = 0, 0.01, 0.05, 0.13, 0.22, 0.29, 0.44$) crystals were grown by modified vertical Bridgman method that provided (0001) crystal plane orientation perpendicular to growth axis. Absorption coefficient is minimal (decreased by up to 3 times) in the THz range at the optimal S-doping of 3 weight % ($x = 0.13$). Increased S content causes the absorption coefficient for e-wave to become frequency independent in the main part of the spectrum from 0.3 to 3 THz. A narrow line-width rigid phonon absorption peak $E''^{(2)}$ at 1.79 THz arises and then declines in intensity with the doping level, in parallel with a shift towards shorter wavelength.

© 2015 Elsevier B.V. All rights reserved.

1. Introduction

Gallium selenide (GaSe) is among the promising nonlinear optical crystals for highly efficient generation of terahertz (THz) radiation. The crystals belong to the $\bar{6}2m$ point group and cleave readily along the {0001} plane. The cleavage is the result of crystal structure consisting of monoatomic layers arranged in planar Se-

Ga-Ga-Se packages [1]. The atomic bonds between planes within these packages are ionic-covalent in nature, while those between the packages are of the weaker Van-der-Waals type. Therefore with careful preparation by a thin blade it is possible to produce optical quality surfaces along this direction [2,3].

However, an access to other crystallographic directions by cutting and polishing is hampered [4,5], since GaSe has perfect cleavage and low hardness [6]. Besides, GaSe possesses low ($0.02 \text{ W/cm}\cdot\text{deg}$) thermal conductivity along the optical axis [1]; often demonstrates limited optical quality (absorption

* Corresponding author.

E-mail address: k.a.kokh@gmail.com (K.A. Kokh).

coefficient $\geq 0.1\text{--}0.2\text{ cm}^{-1}$) due to the presence of point (mainly Ga vacancies [7,8] and micro (Ga inclusions, stacking disorders, broken layers and dislocations) defects; suffers from significant two-photon ($\sim 5 \cdot 10^{-10}\text{ cm}^{-1}/\text{W}$ at $0.755\text{--}0.875\text{ }\mu\text{m}$) and multi-photon absorption under near IR pumping [9,10]; whilst its dislocation density can reach 10^9 cm^{-2} [11], and the fraction of layer stacking faults up to 0.67 [12]. Finally, the available data on GaSe physical properties appear highly scattered.

In order to fully exploit the potential of GaSe and to expand its applications, it is necessary to overcome these limitations. Moderate doping of pure GaSe by various isovalent elements that form isostructural compounds, e.g. sulphur (S), indium (In), tellurium (Te), etc., is an effective way to obtain improvements of the material properties [10,13–22]. It was established that some non-ivalent dopants, such as silver (Ag) [23], that do not form isostructural compounds, or a mixture of isovalent S and non-ivalent Ag [24,25], may also bring improvements in the physical properties of GaSe.

Gallium sulfide (GaS) has a centrosymmetric structure 6/mmm. The range of sulfur solubility in noncentrosymmetric GaSe reaches ~ 20 mol.%; however, the existence of ϵ -polytype was reported to be in the range of $x < 0.03$ [26]. The optical properties of ϵ -GaSe_{1-x}S_x ($0 < x < 0.4$) were studied [14,19], pointing out the higher efficiency of such crystals compared to pure GaSe. This work aims to improve the growth technology of highly doped GaSe by isovalent S anion or growth of solid solution GaSe_{1-x}S_x crystals.

2. Crystal growth

The starting materials for the synthesis were Ga 99.9997, Se 99.99 and S 99.95, which were additionally purified by remelting in a continuously evacuated ampoule. Weighing of the stoichiometric charge of Ga and Se, and nominal 0, 0.3, 1.1, 3, 5, 7, 11 mass.% S or $x = 0, 0.01, 0.05, 0.13, 0.22, 0.29, 0.44$ was performed with the accuracy of ± 0.1 mg. Synthesis ampoules were loaded up to 65% in the volume to minimize the quantity of and interaction with rest gases. Because of high partial pressure of selenium and sulfur, it is impossible to achieve a direct fusion of the components. Usually a two-zone method [27] is used, i.e. evaporation of selenium in the cold zone ($300\text{ }^\circ\text{C}$) and reaction of the vapour with molten gallium in the hot zone ($950\text{ }^\circ\text{C}$). In this work we synthesized the charges in the single-zone furnace reported in [28]. Synthesized polycrystalline material GaSe_{1-x}S_x with various sulfur concentrations is shown in Fig. 1.

For the growth process, the polycrystalline material was loaded into a single wall cylinder ampoule. Crystal growth was performed by the vertical Bridgman method with heat field rotation [29,30]. The growth ampoule was sealed at 10^{-4} torr and loaded into the furnace having a temperature gradient of $\sim 15\text{ K/cm}$ at the estimated level of crystallization front. After homogenization of the melt at the temperature of 30 K above the melting point, the ampoule was mechanically lowered at the speed of 10 mm/day.

The internal surface of the ampoule had a layer of pyrolytic carbon which protected the melt from contact with the walls. As a result, the grown crystal was easily released from the ampoule



Fig. 1. Ampoules with as-synthesised polycrystalline material GaSe_{1-x}S_x, $x = 0.05$ (a) and $x = 0.44$ (b).

without any deformation. If no such coating is applied, the solidified crystal may adhere to the quartz due to chemical reaction.

No seed was used for the following reasons: it is very difficult to prepare a non-deformed seed; layered materials tend to grow along the primary thermal gradient, so most of the crystals were naturally oriented with their (0001) axis along the growth axis. However the orientation of the (0001) plane perpendicular to the growth axis is more favorable, since the preparation of samples becomes simpler. Also, this orientation enables a faster wedging-out of grain boundaries. It was found that heat field rotation may provide the desired growth conditions when the (0001) plane of the crystal was close or orthogonal to the growth axis (Fig. 2a,b).

A visual examination of as-grown crystals showed no color differences between the initial and final parts. The samples were easily cleaved with high quality surfaces up until the end part of the crystals. No eutectic aggregate was found on the top surfaces of the crystal, meaning that all additional components were distributed inside the crystal. This confirms that application of the heat field rotation method [31] is effective in improving convection in the vertical Bridgman technique.

Two types of GaSe_{1-x}S_x samples were fabricated. One type was cleaved from the as-grown boules, i.e. had faces orthogonal to the c-

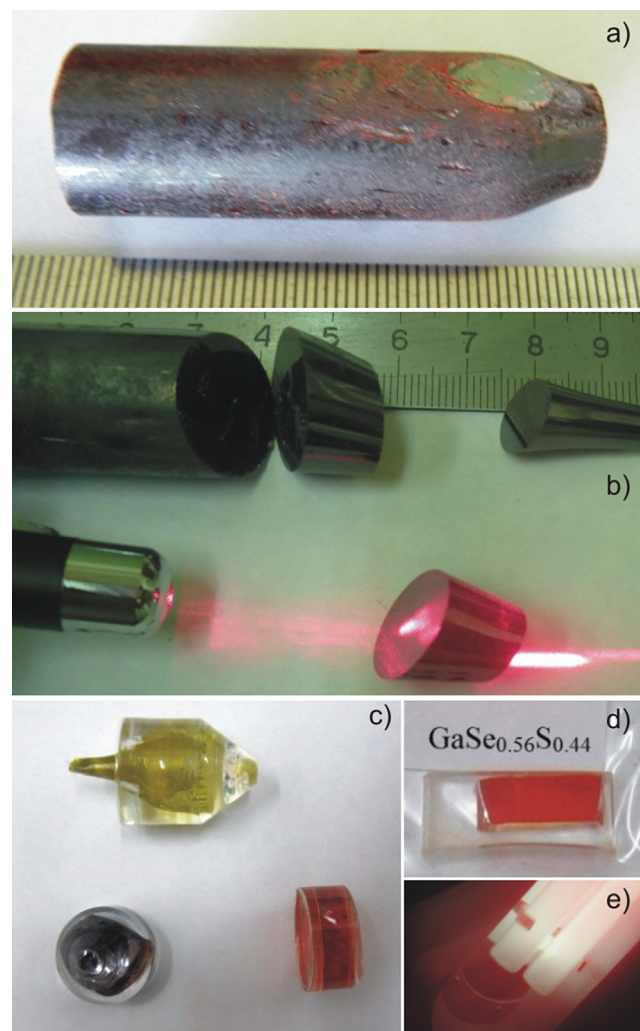


Fig. 2. GaSe:S crystals with the cleavage plane along (a) and perpendicular to (b) the growth axis; (c) GaS (top), GaSe (bottom left) and GaSe_{0.87}S_{0.13} crystals immersed in polymethyl acrylate, (d) a cut and polished 1-mm sample of GaSe_{0.56}S_{0.44} crystal, and (e) view through it at a day-light lamp.

axis, so that a traversing beam travelled parallel to (0001). Its high optical quality can be estimated by the naked eye, evident in its transparency and homogeneity. The second type of sample was mechanically processed (Fig. 2c,d). First, a section of the $\text{GaSe}_{1-x}\text{S}_x$ boule was immersed in a monomer (polymethyl acrylate) mixed with a thermoinitiator and placed in an oven for polymerization for 2 h. Following that, a section was cut perpendicularly to the growth layers and then polished with fine 0.8–1.2 μm POLIRIT polishing powder (48.2 mass.% CeO_2 , 24 mass.% La_2O_3 and 11.3 mass.% NdO_2), so that a traversing beam would travel orthogonally to (0001). For comparison of attenuation properties, some samples were polished with a large diameter (9 μm) polishing powder.

3. Crystal characterization

Scanning electron microscopy (SEM) with a SEM Quanta 200 3D (FEI, Netherlands) microscope was used in the study surface morphology of the samples. This microscope, provided with an EDAX ECON VI micro analyzer, was also used to measure Ga, Se and S contents and to study phase and structural properties. Surface roughness was determined by profilometer Probes HOMMEL-ETAMIC T1000 (JENOPTIK AG, Germany). An X-ray diffractometer Shimadzu XRD 6000 (Japan) and a transmission electron microscope (TEM) CM12 (Philips, Netherlands) were employed in analyzing the structure. UV-visible-near-IR transmission spectra were recorded by a Cary 100 Scan (Varian Inc., Australia) spectrophotometer over the spectral range of 190–900 nm with a spectral resolution of 0.2–4 nm and a wavelength accuracy of ± 1 nm.

The measurements of dispersions of o- and e-wave absorption coefficients in $\text{GaSe}_{1-x}\text{S}_x$ samples in the THz range was carried out

using a Terahertz-Time Domain Spectrometer (THz-TDS) described in detail elsewhere [32,33]. The THz-TDS used a standard configuration incorporating a femtosecond laser, four off-axis parabolic mirrors, a biased GaAs emitter, and electro-optic detection with a (110) ZnTe crystal and balanced Si photodiodes. The frequency resolution was 3.75 GHz. The THz beam was linearly polarised. $\text{GaSe}_{1-x}\text{S}_x$ samples were placed in the focused THz beam such that they interacted with the incident radiation in either $\vec{E} \perp \vec{c}$ (o-wave) configuration in the case of both cleaved and cut & polished samples, or in $\vec{E} \parallel \vec{c}$ (e-wave) configuration in the case of cut & polished samples, where \vec{E} is the electric field vector of the incident light.

4. Results and discussion

The produced samples were free from precipitates, voids or micro bubbles. Cleaved $\text{GaSe}_{1-x}\text{S}_x$ surface (0001) was naturally flat with roughness as low as ≤ 0.15 nm. For cut and polished 1 mm thick samples the measured surface roughness Ra varied from 75 nm for $\text{GaSe}_{0.56}\text{S}_{0.44}$ –220 nm for GaSe samples. Regions of local defects (mainly scratches and cracks along the growth layers) were observed on polished surfaces. It was found that the surface finish of these extremely easily cleaved samples is suitable for THz-TDS study if their thickness is 1 mm or larger. Thinner samples possess high concentrations of cracks and are useless for the study.

The surface morphology with a spatial resolution of 10 μm is depicted in Fig. 3. It was found that the surface quality of the cut & polished samples was suitable for THz-TDS study if their thickness was 1 mm or larger. Thinner samples possess high concentrations of defects (cracks, deformations) and are useless for the study.

No peaks of other elements except Ga and Se were observed in

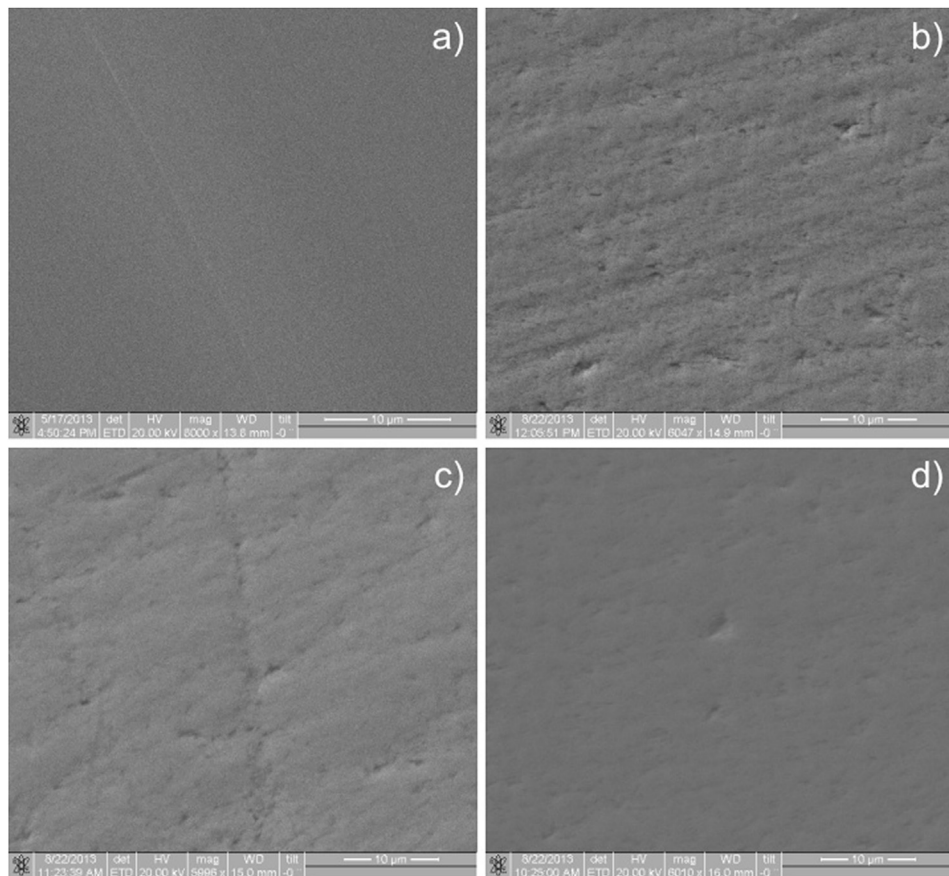


Fig. 3. Morphology of GaSe (0001) cleaved plane (a) and polished surface subperpendicular to (0001) for GaSe (b), $\text{GaSe}_{0.87}\text{S}_{0.13}$ (c) and $\text{GaSe}_{0.56}\text{S}_{0.44}$ (d).

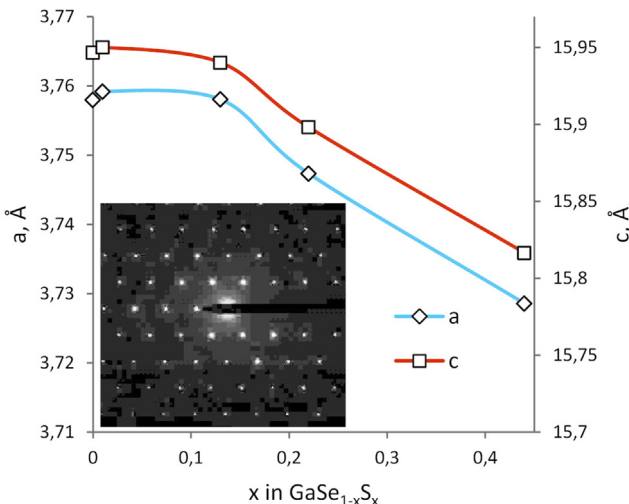


Fig. 4. Lattice parameters versus S-doping for $\text{GaSe}_{1-x}\text{S}_x$ crystals. SAED pattern observed by TEM for $\text{GaSe}_{0.56}\text{S}_{0.44}$ crystal is shown in the figure inset.

the EDAX spectrum indicating the high purity of GaSe. The chemical composition of mixed crystals was close to the charge composition but with as small deviation in sulfur content, below 5 weight %. EDAX spectra recorded by surface scanning confirm the highly uniform distribution of the GaSe composition.

It was found that the powder X-ray diffraction patterns for GaSe are well in coincidence with that in the JCPDS 37-931 card. The lattice structure of all S-doped crystals is still of hexagonal form similar to that for the ϵ -GaSe crystal. The dependence of the lattice parameters a and c of GaSe crystals on S doping, as well as the SAED pattern observed by TEM for $\text{GaSe}_{0.56}\text{S}_{0.44}$, are depicted in Fig. 4. The diffraction pattern clearly confirms the high quality of the crystalline structure of S-doped GaSe crystals up to the mixing ratio $x = 0.44$. The change in lattice parameters does not follow the Vegard's law. A flat dependence for $x < 0.1$ is in agreement with Luo et al. [34]. Such positive deviation from linear dependence is likely to be caused by a nonlinear response of defect concentration to the content of sulfur.

Transformation of Raman scattering spectra with S-doping (Fig. 5) is quite complicated, reflecting the incorporation of sulfur into the GaSe lattice. Well known intense single peaks in GaSe at 312 cm^{-1} and 213 cm^{-1} [35] shift towards shorter wavelength with increasing S content. Some double peaks in solid solution crystals, for example for $\text{GaSe}_{1-x}\text{S}_x$, $x = 0.13$ and 0.22 crystals in Fig. 5, seems to be a superposition of the shifted GaS crystal peak at 300 cm^{-1} and the GaSe peak at 340 cm^{-1} . The shift of intense Raman peaks is always proportional to changes in the number of incorporated S

atoms. It can be proposed that formation of single crystals gives rise to multiplet phonon absorption between 135 and 180 cm^{-1} .

Visible to far-IR (THz) transmission is significantly modified with S doping. In Fig. 6 it is seen that the short-wavelength edge is shifted from 0.62 to $0.54 \mu\text{m}$, thus reducing the two-photon absorption for the Ti:Sapphire laser [30] and removing it totally for the Nd:YAG laser. This fact significantly widens the range of possible applications of $\text{GaSe}_{1-x}\text{S}_x$ crystals. Recorded spectra are well in coincidence with those reported in [36]. The absorption coefficient in the maximal transparency range of 0.6 – $20 \mu\text{m}$ was found to be 0.03 – 0.05 cm^{-1} . These values are as much as 2 – 3 times lower than that measured for crystals of the same composition grown by the conventional Bridgman method.

Selected THz absorption spectra are depicted in Fig. 7. It is difficult to compare THz absorption spectra of the samples that are due to changes in the average absorption properties with the doping level, as they are accompanied by transformation of phonon absorption peaks in both intensity and shifting center frequency. However, it can be determined that the average absorption coefficients for o-wave are higher than for e-wave. This is despite the fact that cut & polished crystals possess excess optical attenuation caused by the processing. In Fig. 6 it is seen that the o-wave absorption coefficient in the $\text{GaSe}_{0.87}\text{S}_{0.13}$ crystal is minimal almost across the whole of the studied frequency range; it is 2 – 3 times smaller than that of the GaSe crystal. The o-wave absorption coefficient in the $\text{GaSe}_{0.87}\text{S}_{0.13}$ crystal was determined to be the lowest among our samples. Therefore S-doping of 3 weight % appears to be the optimal doping level. This is in good agreement with the mid-IR results reported for S-doped crystal in Ref. [14,30] but is in contradiction with the available data for the THz range [37]. Optimal doping was also found from mid-IR data for Er- [21] and Al-doped [20] GaSe crystals, as well as from THz data for Te-doped GaSe crystal [15].

In Fig. 7 it is also seen that the absorption coefficient for e-wave is likewise minimal for the $\text{GaSe}_{0.87}\text{S}_{0.13}$ crystal in the wavelength range 0.3 – 1.0 THz ; while the absorption coefficient for $\text{GaSe}_{0.56}\text{S}_{0.44}$ is characterized by a much weaker frequency dependency. For the first time it was observed that absorption anisotropy, i.e. a difference between o- and e-wave absorption coefficients, declines with increasing S-doping level: in heavier doped crystals the dependence is weaker.

The phonon absorption peak, centered at 1.79 THz and identified as the rigid phonon mode $E''^{(2)}$ was recorded (Fig. 7 inset). It appears with doping, reaches maximum magnitude at the optimal doping level, then becomes vanishingly small at S-doping of 11 weight %. A similar effect was earlier observed in Te-doped GaSe crystal [15], and appears to be a common feature for all GaSe crystals doped with isovalent elements. The existence of optimal doping, the anisotropy of optical absorption in the THz range, and phonon spectra transformation should be taken into account in THz

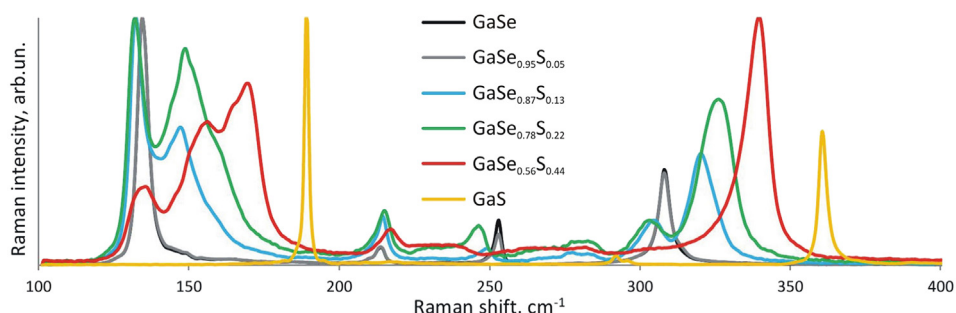


Fig. 5. Raman scattering spectra in GaSe versus S content.

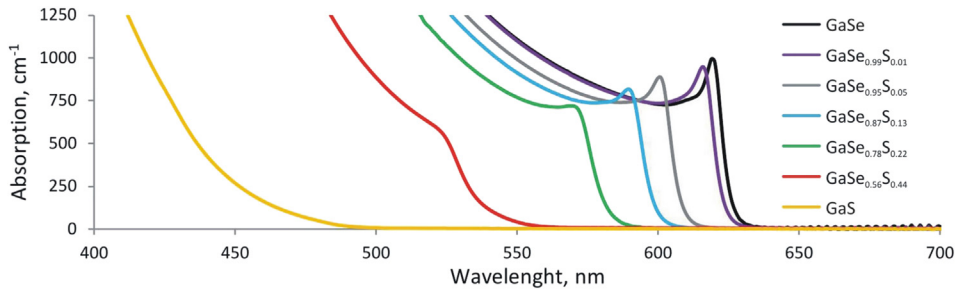


Fig. 6. Short-wavelength absorption edge of GaS, GaSe and $\text{GaSe}_{1-x}\text{S}_x$ crystals in non-polarized light.

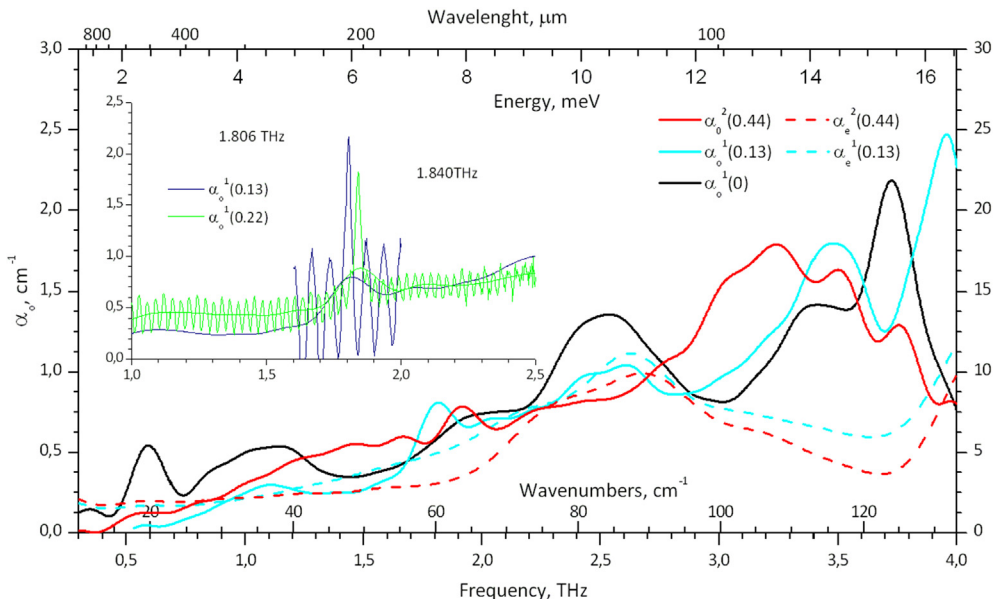


Fig. 7. Smoothed o- and e-wave absorption spectra $\alpha_{0,e}$ for cleaved (right superscript 1) and cut & polished (right superscript 2) $\text{GaSe}_{1-x}\text{S}_x$ crystals with the mixing ratio x shown in brackets. Sections of as-measured spectra with interference patterns and spectral resolution in THz are shown in the figure inset.

applications. It should be emphasized that the average o- and e-wave absorption coefficients for cut & polished crystals are strongly dependent on the particle size of the polishing powder used, the polishing quality, and handling history: crystals polished with powder having 9- μm size grains exhibit an order of magnitude higher optical losses than those polished with 0.8–1.2 μm particles.

5. Conclusion

A set of $\text{GaSe}_{1-x}\text{S}_x$ ($x = 0, 0.01, 0.05, 0.13, 0.22, 0.29, 0.44$) crystals was grown by the modified vertical Bridgman technology that provides growth conditions such that the (0001) plane of crystal lies close or orthogonal to the growth axis. Absorption coefficients for GaSe:S decrease from 2 to 3 times in the IR and THz ranges with increasing S content up to 3 weight % and then rise with further doping. Therefore 3 weight % S-doping has been identified as the optimal doping level for the THz range. At high doping concentrations the absorption coefficient for e-wave becomes almost frequency independent in the main part of the studied 0.3–3 THz range. Absorption anisotropy also decreases with doping. These properties make S-doped GaSe a promising material for THz generation. A narrow line-width absorption peak, identified as a rigid phonon mode $E''^{(2)}$, appears at 1.79 THz, shifts towards shorter wavelengths with doping, and becomes vanishingly small at 11 weight % doping. The results found in this work

can prove useful in selecting the type of three frequency interaction.

Acknowledgements

This work is supported in part by RFBR, Project 12-02-33174. Also the authors acknowledge A.V. Shabalina for SAED patterns. The work at NPL is supported by the National Measurement Office of UK.

References

- [1] N.C. Fernelius, Properties of gallium selenide single crystal, *Prog. Cryst. Growth Charact.* 28 (1994) 275–353.
- [2] K.R. Allakhverdiev, M.O. Yetis, S. Özbeş, T.K. Baykara, E.Yu. Salaev, Effective nonlinear GaSe crystal. Optical properties and applications, *Las. Phys.* 19 (2009) 1092–1104.
- [3] YuM. Andreev, K.A. Kokh, G.V. Lanskii, A.N. Morozov, Structural characterization of pure and doped GaSe by nonlinear optical method, *J. Cryst. Growth* 318 (2011) 1164–1166.
- [4] D.R. Suhre, N.B. Singh, V. Balakrishna, N.C. Fernelius, F.K. Hopkins, Improved crystal quality and harmonic generation in GaSe doped with indium, *Opt. Lett.* 22 (1997) 775–777.
- [5] N.B. Singh, T.B. Norris, T. Buma, R.N. Singh, M. Gottlieb, D. Suhre, J.J. Hawkins, Properties of nonlinear optical crystals in the terahertz wavelength region, *Opt. Eng.* 45 (2006) 094002–094007.
- [6] V.G. Dmitriev, G.G. Gurzadyan, D.N. Nikogosyan, *Handbook for Nonlinear Optical Crystals*, third ed., Springer, Berlin, 1999.
- [7] H. Suzuki, R. Mori, Phase study on binary system GaSe, *Jap. J. Appl. Phys.* 13

- (1974) 417–423.
- [8] V.I. Shtanov, A.A. Komov, M.E. Tamm, D.V. Atrashenko, V.P. Zlomanov, Phase diagram of the gallium selenium system and photoluminescence spectra of GaSe crystals, Dokl. Chem. 361 (1998) 140–144.
- [9] I.B. Zотов, Y.J. Ding, Spectral measurements of two-photon absorption coefficients for CdSe and GaSe crystals, Appl. Opt. 40 (2001) 6654–6658.
- [10] Z.-S. Feng, Z.-H. Kang, F.-G. Wu, J.-Y. Gao, Yu Jiang, H.-Z. Zhang, YuM. Andreev, G.V. Lanskii, V.V. Atuchin, T.A. Gavrilova, SHG in doped GaSe:In crystals, Opt. Express 16 (2008) 9978–9985.
- [11] A. Rizzo, C. de Blasi, M. Catalano, P. Cavaliere, Dislocations in $A^{III}B^{IV}$ crystals, Phys. Stat. Sol. A 105 (1988) 101–112.
- [12] A. Kasuya, Y. Sasaki, S. Hashimoto, Y. Nishina, H. Iwasaki, Stacking fault density and splitting of exciton states in e-GaSe, Sol. State Commun. 55 (1985) 63–66.
- [13] D.R. Suhre, N.B. Singh, V. Balakrishna, N.C. Fernelius, F.K. Hopkins, Improved crystal quality and harmonic generation in GaSe doped with indium, Opt. Lett. 22 (1997) 775–777.
- [14] H.-Z. Zhang, Z.-H. Kang, Yu Jiang, J.-Y. Gao, F.-G. Wu, Z.-S. Feng, YuM. Andreev, G.V. Lanskii, A.N. Morozov, E.I. Sachkova, S.Yu Sarkisov, SHG phase matching in GaSe and mixed $GaSe_{1-x}S_x$, $x \leq 0.412$, crystals at room temperature, Opt. Express 16 (2008) 9951–9957.
- [15] S. Ku, W. Chu, C. Luo, Y. Andreev, G. Lanskii, A. Shaiduko, T. Izaak, V. Svetlichnyi, K. Wu, T. Kobayashi, Optimal Te-doping in GaSe for non-linear applications, Opt. Express 20 (2012) 5029–5037.
- [16] W. Chu, S. Ku, H. Wang, C. Luo, YuM. Andreev, G. Lanskii, T. Kobayashi, Widely linear and non-phase-matched optics-to-THz conversion on GaSe:Te crystals, Opt. Lett. 37 (2012) 945–947.
- [17] Z. Feng, J. Guo, Z. Kang, Y. Jiang, J. Gao, J. Xie, L. Zhang, V. Atuchin, Y. Andreev, G. Lanskii, A. Shaiduko, Tellurium and sulphur doped GaSe for mid-IR applications, Appl. Phys. B Lasers Opt. 108 (2012) 545–552.
- [18] J. Huang, J. Tong, C. Ouyang, J. Chu, Yu Andreev, K. Kokh, G. Lanskii, A. Shaiduko, Intensive terahertz emission from $GaSe_{0.91}S_{0.09}$ under collinear difference frequency generation, Appl. Phys. Lett. 103 (2013), 81104–4.
- [19] J. Guo, D.-J. Li, J.-J. Xie, L.-M. Zhang, Z.-S. Feng, YuM. Andreev, K.A. Kokh, G.V. Lanskii, A.I. Potekaev, A.V. Shaiduko, V.A. Svetlichnyi, Limit pump intensity for sulfur-doped gallium selenide crystals, Laser Phys. Lett. 11 (2014) 055401–055406.
- [20] J. Guo, J.-J. Xie, L.-M. Zhang, D.-J. Li, G.-L. Yang, Yu M. Andreev, K.A. Kokh, G.V. Lanskii, A.V. Shabalina, A.V. Shaiduko, V.A. Svetlichnyi, Characterization of Bridgman grown GaSe:Al crystals, CrystEngComm 15 (2013) 6323–6328.
- [21] Z.-S. Feng, J. Guo, J.-J. Xie, L.-M. Zhang, J.-Y. Gao, YuM. Andreev, T.I. Izaak, K.A. Kokh, G.V. Lanskii, A.V. Shaiduko, A.V. Shabalina, V.A. Svetlichnyi, GaSe:Er crystals for SHG in the infrared spectral range, Opt. Comm. 318 (2014) 205–211.
- [22] Z.-S. Feng, Z.-H. Kang, X.-M. Li, J.-Y. Gao, Yu M. Andreev, V.V. Atuchin, K.A. Kokh, G.V. Lanskii, A.I. Potekaev, A.V. Shaiduko, V.A. Svetlichnyi, Impact of fs and ns pulses on solid solution crystals $Ga_{1-x}In_xSe$ and $GaSe_{1-x}S_x$, AIP Adv. 4 (2014) 037104–037106.
- [23] N.B. Singh, D.R. Suhre, W. Rosch, R. Meyer, M. Marable, N.C. Fernelius, F.K. Hopkins, D.E. Zelmon, R. Narayanan, Modified GaSe crystals for mid-IR applications, J. Cryst. Growth 198 (1999) 588–592.
- [24] Y.-F. Zhang, R. Wang, Z.-H. Kang, L.-L. Qu, Y. Jiang, J.-Y. Gao, YuM. Andreev, G.V. Lanskii, K.A. Kokh, A.N. Morozov, A.V. Shaiduko, V.V. Zuev, AgGaS₂- and Al-doped GaSe crystals for IR applications, Opt. Comm. 284 (2011) 1677–1681.
- [25] J.-J. Xie, J. Guo, L.-M. Zhang, D.-J. Li, G.-L. Yang, F. Chen, K. Jiang, M.E. Evdokimov, M.M. Nazarov, YuM. Andreev, G.V. Lanskii, K.A. Kokh, A.E. Kokh, V.A. Svetlichnyi, Optical properties of non-linear crystal grown from the melt GaSe–AgGaS₂, Opt. Comm. 287 (2013) 145–149.
- [26] A. Gouskov, J. Camassel, L. Gouskov, Growth and characterization of III-VI layered crystals like GaSe, GaTe, InSe, GaSe_{1-x}Te_x and Ga_xIn_{1-x}Se, Prog. Cryst. Growth Charact. 5 (1982) 323–413.
- [27] O. Takahide, N. Yuki, D. Hikari, O. Yutaka, Liquid phase growth of bulk GaSe crystal implemented with the temperature difference method under controlled vapor pressure, J. Cryst. Growth 380 (2013) 18–22.
- [28] J.F. Molloy, M. Naftaly, YuM. Andreev, G.V. Lanskii, I.N. Lapin, A.I. Potekaev, K.A. Kokh, A.V. Shabalina, A.V. Shaiduko, V.A. Svetlichnyi, Dispersion properties of GaS studied by THz-TDS, CrystEngComm 16 (2014) 1995–2000.
- [29] K.A. Kokh, YuM. Andreev, V.A. Svetlichnyi, G.V. Lanskii, A.E. Kokh, Growth of GaSe and GaS single crystals, Cryst. Res. Technol. 46 (2011) 327–330.
- [30] Z.-S. Feng, Z.-H. Kang, X.-M. Li, J.-Y. Gao, Yu M. Andreev, V.V. Atuchin, K.A. Kokh, G.V. Lanskii, A.I. Potekaev, A.V. Shaiduko, V.A. Svetlichnyi, Impact of fs and ns pulses on indium and sulfur doped gallium selenide crystals, AIP Adv. 4 (2014) 037104–037106.
- [31] K.A. Kokh, V.N. Popov, A.E. Kokh, B.A. Krasin, A.I. Nepomnyaschikh, Numerical modeling of melt flows in vertical Bridgman configuration affected by rotating heat field, J. Cryst. Growth 303 (2007) 253–257.
- [32] M. Naftaly, R. Dudley, Methodologies for determining the dynamic ranges and signal-to-noise ratios of terahertz time-domain spectrometers, Opt. Lett. 34 (2009) 1213–1215.
- [33] M. Naftaly, R. Dudley, Linearity calibration of amplitude and power measurements in terahertz systems and detectors, Opt. Lett. 34 (2009) 674–676.
- [34] Z.-W. Luo, X.-A. Gu, W.-C. Zhu, W.-C. Tang, Yu Andreev, G. Lanskii, A. Morozov, V. Zuev, Optical properties of GaSe:S crystals in terahertz frequency range, Opt. Precis. Eng. 19 (2011) 354–359.
- [35] K. Allakhverdiev, T. Baykara, S. Ellialtioglu, F. Hashimzade, D. Huseinova, K. Kawamura, A.A. Kaya, A.M. Kulibekov, S. Onari, Lattice vibrations of pure and doped GaSe, Mat. Res. Bull. 41 (2006) 751–763.
- [36] E. Cuculescu, I. Evtdiev, I. Caraman, The anisotropy of the optical properties of ternary semiconductors formed by elements of III and VI groups, Phys. Stat. Sol. B 6 (2009) 1207–1212.
- [37] S.Yu Sarkisov, M.M. Nazarov, A.P. Shkurinov, O.P. Tolbanov, GaSe_{1-x}S_x and GaSe_{1-x}Te_x solid solutions for terahertz generation and detection, in: Proc. of the 34th Int. Conf. on Infrared, Millimeter and Terahertz Wave (IRMMW-THz-2009), 21–25 September, 2009, Busan, Korea. Paper M1A02.0370. ISSN: ISBN 978-1-4244-5417, IEEE catalog # CFPO91MM-CDR.